Attenuated herpes simplex virus 1 blocks arterial apoptosis and intimal hyperplasia induced by balloon angioplasty and reduced blood flow

Christopher L. Skelly*†, Amito Chandiwal*, James E. Vosicky*, Ralph R. Weichselbaum‡, and Bernard Roizman§¶

*Section of Vascular Surgery, Department of Surgery, ‡Department of Radiation and Cellular Oncology, and §Marjorie B. Kovler Viral Oncology Laboratories, University of Chicago, Chicago, IL 60637

Contributed by Bernard Roizman, June 9, 2007 (sent for review May 24, 2007)

Injury caused by distention of the arterial wall by balloon angioplasty can result in apoptosis and vascular smooth muscle cell proliferation. Here, we report that a brief exposure of the arterial lumen to a genetically engineered, attenuated herpes simplex virus 1 blocks activation of caspase 3-dependent apoptosis and MAPK-dependent cell proliferation induced by carotid artery balloon angioplasty and ligation to reduce blood flow. The procedure enables the restoration of the endothelial cell layer lining the lumen and prevents neointimal hyperplasia and restenosis. These findings have a broad application in prevention of balloon angioplasty-induced restenosis.

neointimal hyperplasia | restenosis | vascular smooth muscle cells | endothelial cells

Approximately 80 million people suffer from cardiovascular disease, and nearly 1.3 million angioplasty and stent procedures are performed annually (1). Patients with short- as well as long-segment occlusive atherosclerotic lesions of most major arteries are treated increasingly by endovascular intervention with percutaneous transluminal angioplasty and selective stent placement. The efficacy of intravascular stents is compromised by the natural response of blood vessels to injury and by hemodynamic alterations in the artery. Both angioplasty and bare metal stents are associated with significant restenosis caused by neointimal hyperplasia that leads to a 14% incidence of reintervention (2). Recent reports have described late in-stent thrombosis in drug-eluting stents (3, 4).

Arterial remodeling is a natural response of blood vessels to injury and to altered hemodynamics secondary to stent placement. The response is multifaceted and includes inflammation (5), vascular smooth muscle cell proliferation and migration, and apoptosis (6). The resulting neointimal hyperplasia is a predominant cause of arterial restenosis after percutaneous interventions.

The objective of the studies reported here was to test the hypothesis that intimal hyperplasia results from an intravascular injury. We tested whether injury leads to programmed cell death, which, in turn, induces division of surviving cells. To test this hypothesis, we used a herpes simplex virus 1 (HSV-1) mutant R7020 that has been shown to be safe in both preclinical and clinical studies (7, ‖). A corollary of the hypothesis tested is that the mutant virus selected for these studies would block both apoptosis and neointimal proliferation. We report that, in a rabbit model of carotid artery balloon angioplasty and ligation-induced blood flow reduction, exposure of the artery for a brief interval to one such mutant prevented apoptosis and neointimal hyperplasia in injured tissues.

The following points are relevant to this report. In recent years, genetically engineered, highly attenuated HSV-1 mutants have been studied extensively for therapy of malignant tumors of the central nervous system (8–12) and liver (7). Moreover, such mutants have been shown to infect and express genes in vascular smooth muscle cells *in situ* (13). A characteristic of these attenuated HSV-1 mutants is that they preferentially infect and multiply in dividing cells. In addition, HSV-1 encodes at least three genes, each of which blocks apoptosis; these genes have not been deleted in mutants tested in clinical trials to date. The genes are US3, US5, and US6 encoding a protein kinase and the glycoproteins J and D, respectively (reviewed in ref. 14).

HSV-1 DNA consists of two stretches of unique sequences flanked by inverted repeats. The HSV-1 mutant R7020 used in these studies to modify the intravascular response to injury was designed as a candidate for prophylactic immunization against HSV-1 and HSV-2 infection (‖, 15, 16). The mutant lacks a portion of the UL23 (thymidine kinase) and UL24 genes. In place of the internal inverted repeats encoding one copy each of the $\alpha 0$, $\alpha 4$, and $\gamma_1 34.5$ genes and the unique UL56 gene, the virus carries the HSV-1 genes encoding US4, US5, US6, and US7 as well as a potion of US8 and an intact copy of the HSV-1 thymidine kinase gene driven by the $\alpha 4$ promoter.

Results

The Genetically Engineered R7020 Virus Mutant Blocks Neointimal Hyperplasia in the Carotid Artery of New Zealand White Rabbits After Balloon Angioplasty and Ligation-Induced Blood Flow Reduction. In this series of experiments, New Zealand White rabbits in groups of eight animals per procedure were treated as follows. Group 1 was subjected to sham surgery (sham group). Group 2 was subjected to balloon angioplasty injury and carotid ligation to reduce blood flow, followed by 10 min of intrarterial exposure to buffered saline (control group). Group 3 was subjected to balloon angioplasty injury and carotid ligation to reduce blood flow, followed by 10 min of intrarterial exposure to R7020 in buffered saline (treated group). The procedures were as described in *Materials and Methods*. The animals recovered from their procedure, and the experiments were terminated after 3, 14, or 28 days. The animals were killed humanely, and the carotid arteries were excised and subjected to analyses described in *Materials and Methods*. Representative cross-sections of arteries excised in this experiment are shown in Fig. 1. The histological measurements are summarized in Table 1. In summary, no vessel was occluded at the termination of the experiment. The brief

Author contributions: C.L.S., R.R.W., and B.R. designed research; C.L.S., A.C., and J.E.V. performed research; R.R.W. and B.R. contributed new reagents/analytic tools; C.L.S. and R.R.W. analyzed data; and C.L.S. and B.R. wrote the paper.

The authors declare no conflict of interest.

Abbreviations: HSV-1, herpes simplex virus 1; PCNA, proliferating cell nuclear antigen; CCA, common carotid artery.

†To whom correspondence may be addressed at: Section of Vascular Surgery, Department of Surgery, University of Chicago, MC 5028, 5841 South Maryland Avenue, Chicago, IL 60637. E-mail: cskelly@surgery.bsd.uchicago.edu.

¶To whom correspondence may be addressed. E-mail: bernard.roizman@bsd.uchicago.edu.

‖Cadoz, M., Micoud, M., Seigneurim, J. M., Mallert, M. R., Baccard, C., Moranbd, P., 32nd Interscience Conference on Antimicrobial Agents and Chemotherapy, October 11–14, 1992, Anaheim, CA.

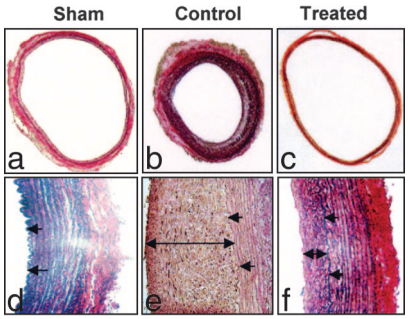

Fig. 1. Weigert Van Gieson staining of the left CCA at 4 weeks in sham ($n = 4$), control ($n = 4$) (CCA subjected to balloon injury with three passes of 3F balloon catheter, exposed intraluminally to PBS, and then restricted by ligating over a 0.014 guide wire distal to the cranial thyroid branch to create a low shear stress and low flow environment), and HSV-1 R7020-treated group ($n = 4$) (CCA subjected to balloon injury with three passes of 3F balloon catheter, exposed intraluminally to HSV-1 R7020 mutant for 10 min at a titer of 1×10^9 pfu/ml, and then restricted over a 0.014 guide wire as in the controls). The single arrow represents the internal elastic lamina of the CCA, and the double arrow depicts the neointimal thickening (NIT). (Magnification: *a–c*, ×4; *d–f*, ×40.)

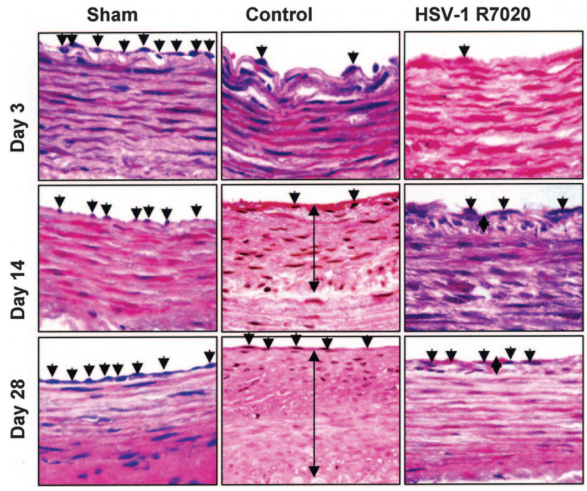

Fig. 2. H&E staining of representative sections of the CCA at 3, 14, and 28 days in sham ($n = 8$), control ($n = 8$), and HSV-1 R7020-treated ($n = 8$) groups. A single arrow represents the endothelial cells of the CCA, and the double arrow depicts the neointimal thickening (NIT).

exposure of the artery to the R7020 resulted in a significant reduction in neointimal hyperplasia (56 ± 9 μm vs. 176 ± 17 μm; $P < 0.05$) and medial thickness (99 ± 10 μm vs. 220 ± 10 μm; $P < 0.05$) compared with control. As expected, there were no changes in the intima of the carotid arteries of the sham group. The intima/media ratio and wall thicknesses were also greater in the control group compared with those of the treated and sham groups. These results demonstrate the efficacy of R7020 in preventing neointimal hyperplasia resulting from balloon injury coupled with reduced blood flow.

The Integrity of the Endothelial Cell Layer Lining the Carotid Artery Subjected to Injury by Balloon Angioplasty and Reduced Blood Flow Was Restored in R7020-Treated Animals. One undesirable, yet expected, outcome of angioplasty and stent placement is the formation of scar tissue and disruption of the endothelial layer. The results of analyses of the histological sections described in *Materials and Methods* and illustrated in Fig. 2 were as follows. The endothelial cell layer was largely denuded from artery that was subjected to balloon angioplasty and reduced blood flow in both control animals and virus-treated animals, as noted at day 3. The endothelial layer was restored partially after 14 days and was restored completely 28 days after the balloon angioplasty and ligation in both the control and the R7020 mutant virus-treated arteries. We conclude that the exposure of arterial wall to the mutant virus had no effect on the regeneration of the endothelial cells lining the luminal wall.

Genetically Engineered Mutant Virus R7020 Blocks Activation of Caspase 3, MAPKs ERK1/2, and Proliferating Cell Nuclear Antigen (PCNA) After Balloon Angioplasty and Ligation-Induced Blood Flow Reduction. Consistent with the hypothesis underlying these studies, in this series of experiments, we examined the status of four markers in arteries 3 and 14 days after surgery. These markers were (*i*) activated caspase 3 and accumulation of cleaved DNA fragments (TUNEL assay), markers of cells undergoing apoptosis, and (*ii*) activated ERK1/2 and accumulation of PCNA, markers of cellular proliferation in arterial walls. Two series of measurements were done. In the first series, the arteries were examined by immunohistochemistry for caspase 3, DNA fragmentation (TUNEL), or accumulation of PCNA as described in *Materials and Methods*. In the second series, the arteries were solublized. The lysed tissues were separated electrophoretically and reacted with antibodies against activated caspase 3, ERK1/2, and PCNA. The amounts of caspase 3, ERK1/2, or PCNA were determined by normalization of the amounts detected in these assays with respect to the amounts of GAPDH. The procedures were as described in *Materials and Methods*. The results were as follows:

1. Fourteen days after surgery, none of the arteries examined in this study was positive in TUNEL assays for DNA fragmentation, activation of caspase 3, accumulation of ERK1/2, or PCNA. Three days after surgery, DNA fragmentation, activated caspase 3, and accumulation of ERK1/2 and PCNA were detected.
2. Representative images of the immunohistologic analyses on arteries removed 3 days after surgery are shown in Fig. 3. Fig. 4 shows estimates of the average area of the intima and media containing cells with activated caspase 3, fragmented DNA (TUNEL), or PCNA. Immunohistologic analyses indicated that a significant portion of the intima and media of control (40–50%) arteries contained cells with detectable amounts of activated caspase 3, fragmented DNA accumulation, and PCNA. In contrast, the areas of intima and media in the

Table 1. Carotid artery morphometry at 4 weeks

Group	*n*	Neointimal thickness, μm	Medial thickness, μm	I/M ratio	Luminal radius, mm	Luminal area, mm^2
Sham	4	0*	146 ± 18	0	1.40 ± 0.11	6.24 ± 0.96
Control	4	$176 \pm 17^{\dagger}$	$220 \pm 10^{\dagger}$	$0.8 \pm 0.09^{\dagger}$	1.23 ± 0.05	4.8 ± 0.39
HSV-1-treated	4	$56 \pm 9^{\dagger\ddagger}$	$99 \pm 10^{\ddagger}$	$0.55 \pm 0.04^{\dagger\ddagger}$	$1.91 \pm 0.09^{\dagger\ddagger}$	$11.49 \pm 1.05^{\dagger\ddagger}$

Data are expressed as means ± SEM. I/M, intima/media; *, thickness too small to be measured accurately; †, $P < 0.05$ compared with sham; ‡, $P < 0.05$ compared with control.

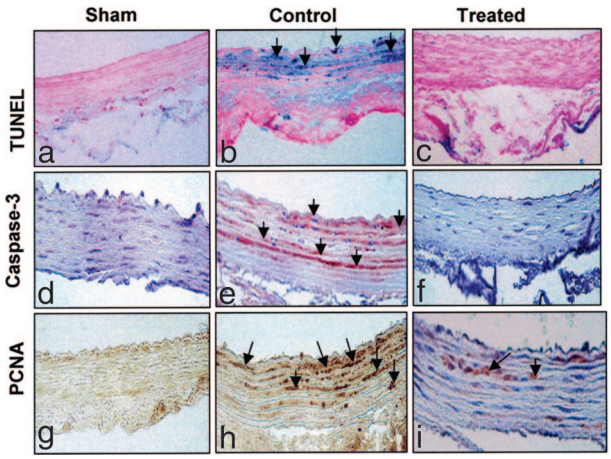

Fig. 3. HSV-1 R7020 mutant blocks flow and mechanically induced apoptosis. Immunohistochemical analysis of the left CCA at 3 days in sham (*a*, *d*, and *g*), control (*b*, *e*, and *h*), and HSV-1 R7020-treated (*c*, *f*, and *i*) groups. Detection of apoptosis was performed by TUNEL assay (*a*–*c*) using the VasoTACS *in situ* apoptosis detection kit per the manufacturer's instructions. Detection of cleaved caspase 3 (*d*–*f*), one of the key executioners of apoptosis, was performed by using a SignalStain IHC detection kit. Cell proliferation was assessed by PCNA staining (*g*–*i*).

virus-treated arteries exhibited active caspase 3, PCNA, and fragmented DNA that was ≈10% for virus-treated arteries and ≈5% in sham-treated arteries.

3. The immunoblotting studies shown in Fig. 5 yielded consistent results. All three markers tested (ERK1/2, PCNA, and activated caspase 3) were virtually undetectable in sham-treated arteries but were highly elevated in control arteries. A striking feature of the results is the very low levels of ERK1/2 and PCNA detected in virus-treated arteries and greatly reduced levels of activated caspase 3.

The results indicate that, at the time tested (3 days after surgery), the vascular smooth muscle cell proliferation, which was prevalent in control arteries, was absent or very low in the R7020-treated arteries.

Discussion

The salient features of the results presented in this study may be summarized as follows. Distention of the arterial wall by balloon angioplasty and reduced blood flow leads to intimal hyperplasia. In the initial stages, two seemingly contradictory processes take place. First, two independent assays indicate that, 3 days after the balloon angioplasty and reduced blood flow, a significant area of the intima and media contain cells undergoing apoptosis. Concurrently, the results show that an equally significant portion of the intima and media contains cells undergoing proliferation as indicated by the accumulation of PCNA and MAPK ERK1/2. In addition, the endothelial cell layer lining the arterial lumen is largely denuded. It is tempting to speculate that the distention of the arterial wall by the balloon angioplasty damaged the endothelial layer and resulted in apoptosis of underlying cells. This, in turn, induced proliferation of surviving cells. Finally, reduced blood flow led to an overcompensation of dividing cells and restenosis. A key conclusion of the studies on control animals is that the response to angioplasty and reduced blood flow took place soon after surgery, and, therefore, any intervention to block restenosis must be applied at that time or soon after angioplasty. By day 3, we observed both apoptotic cells and proliferating cells as measured by the respective markers.

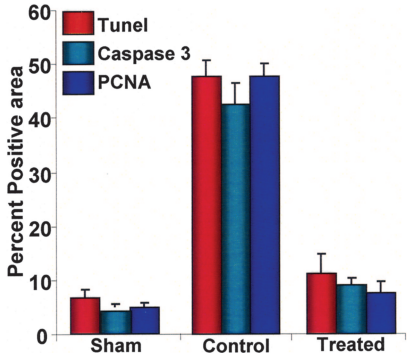

Fig. 4. Regions with positive TUNEL, caspase-3, and PCNA staining were evaluated by using Image J as described in *Materials and Methods*.

The brief exposure of the damaged artery to the R7020 mutant virus resulted in a dramatic decrease in the relative numbers of apoptotic cells concurrent with a decrease in the amounts of active caspase 3 detected in the virus-treated arteries. At the same time, we detected a decrease in amount of proteins characteristic of proliferating cells (PCNA, ERK1/2).

Finally, the results indicated that, at 28 days after the surgery, the endothelial layers of both control and virus-treated arteries were fully restored and intact. The difference, however, is that in control arteries, the thickness of the intima was significantly greater than that of sham-treated or virus-treated arteries.

A Central Issue Is the Mechanisms by Which HSV-1 Mutants Like R7020 Block Restenosis. The salient property of this mutant is that it does not replicate effectively in normal, nondividing cells. We propose that the virus infects the cells injured by the angioplasty and blocks initiation of apoptosis. This, in turn, would reduce the stimulus for cell proliferation, and, most likely, the virus also is infecting the cells undergoing division. Both the reduction of the number of apoptotic cells and the propensity of R7020 to replicate in dividing cells most likely account for the inhibition of restenosis. A positive feature of the R7020 mutant is that its thymidine kinase gene is driven by a much more potent viral promoter than the native promoter, ensuring greater and quicker inhibition of viral replication if it is so desired.

The studies described in this and preceding reports suggest that mutants with properties like those of R7020 (and safety profiles similar to R7020) may have a significant impact on the outcomes of angioplasty performed in humans without affecting the work flow of the surgical intervention. The use of a balloon to temporarily restrict the blood flow enables the virus to be targeted to diseased areas of the artery.

Materials and Methods

Animal Operations. Animals were cared for in accordance with the University of Chicago Institutional Animal Care and Use Committee. Male New Zealand white rabbits (3 kg) were anesthetized with an i.m. injection of 40 mg/kg ketamine hydrochloride and 5 mg/kg xylazine augmented with 1–3% isoflurane titrated for effect via endotracheal intubation. Antibiotic prophylaxis was provided with 10 mg/kg enrofloxacin i.m. daily for 3 days. Aspirin at 1 mg/kg and 25 mg/kg clopidogrel dissolved in water were given as a loading dose 24 h before surgery, and a maintenance dose (1 mg/kg aspirin and 10 mg/kg clopidogrel) was continued until termination of the experiments at either 3, 14, or 28 days to reduce the incidence of thrombus formation. Intraarterial pressure was monitored through a 22-gauge cannula placed in the contralateral ear artery.

Animal Model. For all of the animal groups, a 4-cm length of left common carotid artery (CCA) was exposed after surgical incision overlying the anterior border of sternocleidomastoid muscle was performed. Systemic anticoagulation was achieved with 200

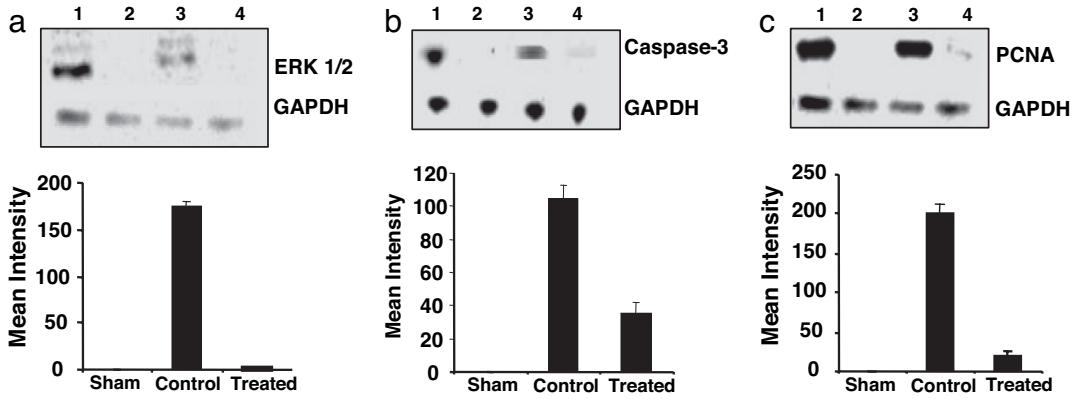

Fig. 5. Immunoblot analysis of the left CCA with densitometry analysis for ERK 1/2 (*a*), caspase-3 (*b*), and PCNA (*c*) at 3 days in positive control (lane 1), sham (lane 2), control (lane 3) and HSV-1 R7020-treated (lane 4) groups.

units/kg of heparin. Proximal and distal control of the left CCA was obtained, and a transverse arteriotomy was made just distal to the craniothyroid branch. A 3F Fogarty balloon catheter (Edwards Lifesciences, Irvine, CA) then was inserted retrograde into the CCA. The balloon catheter then was inflated with 0.1 ml of isotonic saline solution (1.1:1 balloon/artery ratio), and the inflated catheter was withdrawn in a stepwise fashion to the entry point. The procedure was repeated a total of three times to create a 3- to 4-cm area of balloon injury. A cannula then was inserted, and the segment of artery was irrigated with 1 ml of PBS (control group, $n = 8$) or 1 ml of PBS with 1×10^9 pfu/ml HSV-1 (treated group, $n = 8$) at a mean pressure of 80 mmHg (1 mmHg = 133 Pa) for 10 min. The irrigant then was withdrawn, and the CCA was restricted by ligating distal to the cranial thyroid branch over an 0.014 guide wire, leaving a restricted lumen to sustain some measure of outflow in addition to the cranial thyroid branch. The arteriotomy then was repaired by using 8-0 nonabsorbable prolene surgical suture (TE-145; Davis-Geck, Manatee, Puerto Rico) under 4.3× loupe magnification. The clamps were released, and blood flow was restored. Hemodynamic measurements were performed. The incision was closed in two layers with 3-0 vicryl suture (s.c. tissue) and 3-0 nylon suture (skin). Anticoagulation was not reversed, and the endotracheal tube was removed. The animal was allowed to recover. For the sham group ($n = 8$), the left CCA was exposed temporally as for the other groups, and the skin was sutured closed as the others were.

After 3, 14, or 28 days, the animals were reanesthesized, and the injured CCA segments were reexposed by using the same methods of anesthesia and surgical sterility previously described. Repeat flow and pressure measurements were made, and the animals were humanely killed by using 120 mg/kg i.v. pentobarbital. Segments (4 cm) of injured artery were harvested from each rabbit. The artery was perfusion-fixed with 1.25% formaldehyde at the last recorded systemic blood pressure for 10 min. The proximal half of the segment was used for protein analysis and was snap-frozen in liquid nitrogen. The distal segment then was divided into segments of ≈6 mm, each representing proximal, middle, and distal portions, sectioned on the cryostat, and stained with both H&E staining and Weigert van Geisson's elastic tissue stain for histology.

Flow and Pressure Monitoring and Hemodynamic Assessment. Simultaneous pressure and flow waveforms in the artery were measured after exposing the CCA and after restriction and arteriotomy repair of the CCA with an Transonic flow probe (2SB; Transonics Systems, Ithaca, NY) and an ultrasonic transit-time flow meter (HT207; Transonics Systems). Simultaneous pressure and flow waveforms were recorded with a digital data acquisition system (Lab Master DMA; Scientific Solutions, Solon, OH). Length of the CCA balloon that was injured and external diameter were measured with digital calipers (CD-6; Mitutoyo Corporation, Osaka, Japan). Measured hemodynamic variables included pressure and blood flow.

Immunohistochemistry. Sections (5 μm) prepared from paraffin-embedded, longitudinally cut tissue samples of the CCA at day 3 from the sham, control, and HSV-1-treated groups were used for immunohistochemistry. Briefly, the sections were deparaffinized and rehydrated in a descending alcohol series.

Detection of apoptosis was performed by TUNEL assay using the VasoTACS *in situ* apoptosis detection kit (Trevigen, Gaithersburg, MD). The sections were incubated with proteinase K (Trevigen), washed with deionized water, incubated with 3% H_2O_2 for 5 min, and washed with deionized water again. TUNEL staining was performed as per the manufacturer's instructions.

Detection of cleaved caspase 3, one of the key executioners of apoptosis, was performed by using a SignalStain IHC detection kit (Cell Signaling, Danvers, MA). Antigen unmasking was done by immersing slides in 0.01 M sodium citrate buffer followed by peroxidase quenching to block endogenous peroxidase activity. To prevent nonspecific binding, the sections were immersed in a blocking solution for 1 h at room temperature. For antibody staining, sections first were incubated with a prediluted primary antibody at 4°C overnight, rinsed for 15 min with PBS, incubated with biotinylated secondary antibody for 30 min at room temperature, and rinsed for a further 15 min with PBS. The sections then were stained per the manufacturer's protocol and counterstained with hematoxylin.

Cell proliferation was assessed by staining for PCNA to look for the actively cycling cells within the media and intima. After antigen unmasking and peroxidase quenching as described above, the sections incubated in a blocking solution to prevent nonspecific binding. Sections then were incubated with anti-PCNA (1:100 dilution, Nova Biochem, La Jolla, CA) at room temperature for 1 h, rinsed with PBS and incubated with a biotinylated secondary antibody (anti-mouse IgG; Vector Laboratories, Burlingame, CA) for 30 min at room temperature followed by washing with PBS. The sections then were incubated with the ABC reagent (avidin-biotin complex; Vector Laboratories) for 1 h at room temperature and incubated with diaminobenzidine. The reaction was analyzed under a microscope, and the slides were rinsed when brown precipitate developed, indicating positive staining. Counterstain with methyl green was applied before placing a coverslip.

Immunoblotting. After perfusion fixation with 1.25% glutaraldehyde, the left CCA was excised, snap-frozen in liquid nitrogen, and morselized via mortar and pestle with subsequent homogenization on ice in lysis buffer containing 20 mM Hepes (pH 7.4), 2 mM EDTA, 1 mM DTT, 1 mM Na_3VO_4, 1% Triton X-100, 10% glycerol, 2 μM leupeptin, 400 μM PMSF, and 10 units/ml aprotinin (Sigma, St. Louis, MO). The homogenate was incubated for 30 min at 4°C and then centrifuged at 10,000 $\times$ *g* for 10 min at 4°C. The supernatant was removed, and protein concentration was determined by using the Bradford method. Equal amounts of each protein extract (50 μg per lane) were heated at 95°C for 10 min in sample buffer (94 mM phosphate buffer, pH 7.0/1% SDS/2 M urea/3% 2-mercaptoethanol) and then separated onto SDS/10% PAGE under reducing conditions and transferred to nitrocellulose membrane (Millipore, Bedford, MA) in a Novex Western transfer apparatus (Invitrogen, Carlsbad, CA) per the manufacturer's instructions. The blots were washed and incubated with anti-caspase 3 rabbit polyclonal primary antibody (Calbiochem, San Diego, CA) and anti-rabbit secondary antibody (PierceBiotechnology, Rockford, IL) for detection of caspase 3. For detection of PCNA, HRP-conjugated mouse mAb specific for PCNA (Dako, Carpinteria, CA) was used. For ERK 1/2, mouse mAb (sc-7383; Santa Cruz Biotechnology, Santa Cruz, CA) was used. GAPDH Ab (Chemicon, Temecula, CA) was used a loading control. The blots were developed with an ECL Western blotting system (Amersham Biosciences, Piscataway, NJ), and densitometry analysis was performed by using a KODAK (Rochester, NY) Image Station 440cf system.

Image Analysis. For evaluating regions with positive TUNEL, caspase 3, and PCNA staining, ImageJ, a processing and analysis software, was used, as described previously (17). In brief, digital images were acquired with a microscope equipped with a 3.0-megapixel digital camera (Olympus; Melville, NY). The regions of interest were photographed in 8-bit grayscale at a magnification of $\times$4, the backgrounds were normalized, and the density thresholds were set to 130 (minimum) and 255 (maximum). The image then was inverted to give the positive staining as red on a black background. A region of 0.04 mm^2 was selected to measure the positive area in eight equidistant regions on the section in both media and adventitia. Analysis was performed by using the ImageJ particle analysis algorithm. The percent positive area was calculated by dividing the positive staining area by the total area (0.04 mm^2) of the region selected. For each region of interest, a spot check was performed by visually counting the cells under the microscope, and the consistency of results obtained with both methods was found to exceed 95%.

Histology and Assessment of Morphology. After 4 weeks, the operated left CCA was reexposed as previously described. Blood pressure and blood flow were measured and recorded as described above. The proximal CCA was cannulated with an olive-tipped catheter, and the distal CCA and the cranial thyroid branch were clamped, the artery perfusion was fixed with 1.25% glutaraldehyde at 80 mmHg for 10 min, and the CCA was excised. Sections (5 μm) were then cut and stained with the Weigert van Gieson or H&E stains. Sections of each specimen were analyzed histomorphometrically in a blinded fashion. Digital images were acquired with a microscope equipped with a 3.0-megapixel digital camera (Olympus). Neointimal and medial thickness were digitally measured by using Image Pro Plus software (Media Cybernetics; Silver Spring, MD), and the intima/media ratio and the wall thickness were calculated by using the neointimal and medial thickness. Luminal area was used to calculate the luminal radius for all of the different groups.

Data Analysis. Data analysis was performed by using standard software (SPSS 8.0; SPSS, Chicago, IL). Data are presented as means $\pm$ SEM. Comparison of means was achieved by using one-way ANOVA with Tukey's honestly significant differences test, and significance was assigned at $P < 0.05$.

C.L.S. was supported by American Heart Association Scientist Development Grant 0635202N and by an American College of Surgeons Faculty Research Fellowship.

1. American Heart Association (2007) *Heart Disease and Stroke Statistics: 2007 Update* (Am Heart Assoc, Dallas). Available at http://www.americanheart.org/downloadable/heart/1166711577754HS_StatsInsideText.pdf. Accessed April 2, 2007.
2. Williams DO, Holubkov R, Yeh W, Bourassa MG, Al-Bassam M, Block PC, Coady P, Cohen H, Cowley M, Dorros G, *et al*. (2000) *Circulation* 102:2910–2914.
3. McFadden EP, Stabile E, Regar E, Cheneau E, Ong AT, Kinnaird T,Suddath WO, Weissman NJ, Torguson R, Kent KM, *et al.* (2004) *Lancet* 236:1519–2151.
4. Kuchulakanti PK, Chu WW, Torguson R, Ohlmann P, Rha SW, Clavijo LC, Kim SW, Bui A, Gevorkian N, Xue Z, *et al.* (2006) *Circulation* 113:1108–1113.
5. Hanke H, Hassenstein S, Ulmer A, Kamenz J, Oberhoff M, Haase KK, Baumbach A, Gown AM, Karsch KR (1994) *Eur Heart J* 15:691–698.
6. Clowes AW, Reidy MA, Clowes MM (1983) *Lab Invest* 49:208–215.
7. Kemeny N, Brown K, Covey A, Kim T, Bhargava A, Brody L, Guilfoyle B, Haag NP, Karrasch M, Glassschroeder B, *et al.* (2006) *Hum Gene Ther* 17:1214–1224.
8. Harrow S, Papanastassiou V, Harland J, Mabbs R, Petty R, Fraser M, Hadley D, Patterson J, Brown SM, Rampling R (2004) *Gene Ther* 11:1648–1658.
9. Detta A, Harland J, Hanif I, Brown SM, Cruickshank GJ (2003) *Gene Med* 5:681–689.
10. Shah AC, Benos D, Gillespie GY, Markert JM (2003) *J Neuro-Oncol* 65:203–226.
11. Papanastassiou V, Rampling R, Fraser M, Petty R, Hadley D, Nicoll J, Harland J, Mabbs R, Brown SM (2002) *Gene Ther* 9:398–406.
12. Markert JM, Medlock MD, Rabkin SD, Gillespie GY, Todo T, Hunter WD, Palmer CA, Feigenbaum F, Tornatore C, Tufaro F, *et al.* (2000) *Gene Ther* 7:859–866.
13. Skelly CL, Curi MA, Meyerson SL, Woo DH, Hari D, Vosicky JE, Advani SJ, Mauceri HJ, Glagov S, Roizman B, *et al.* (2001) *Gene Ther* 8:1840–1846.
14. Roizman B, Knipe DM, Whitley RJ (2007) in *Fields' Virology*, eds Knipe DM, Howley P, Griffin DE, Lamb RA, Martin A, Roizman B, Straus SE (Lippincott, New York), 5th Ed, pp 2501–2601.
15. Meigner B, Longnecker R, Roizman B (1988) *J Infect Dis* 158:602–614.
16. Meigner B, Longnecker R, Roizman B (1990) *J Infect Dis* 162:313–321.
17. Ide M, Jimbo M, Yamamoto M, Kubo O (1997) *Neurol Med Chir (Tokyo)* 37:158–162.